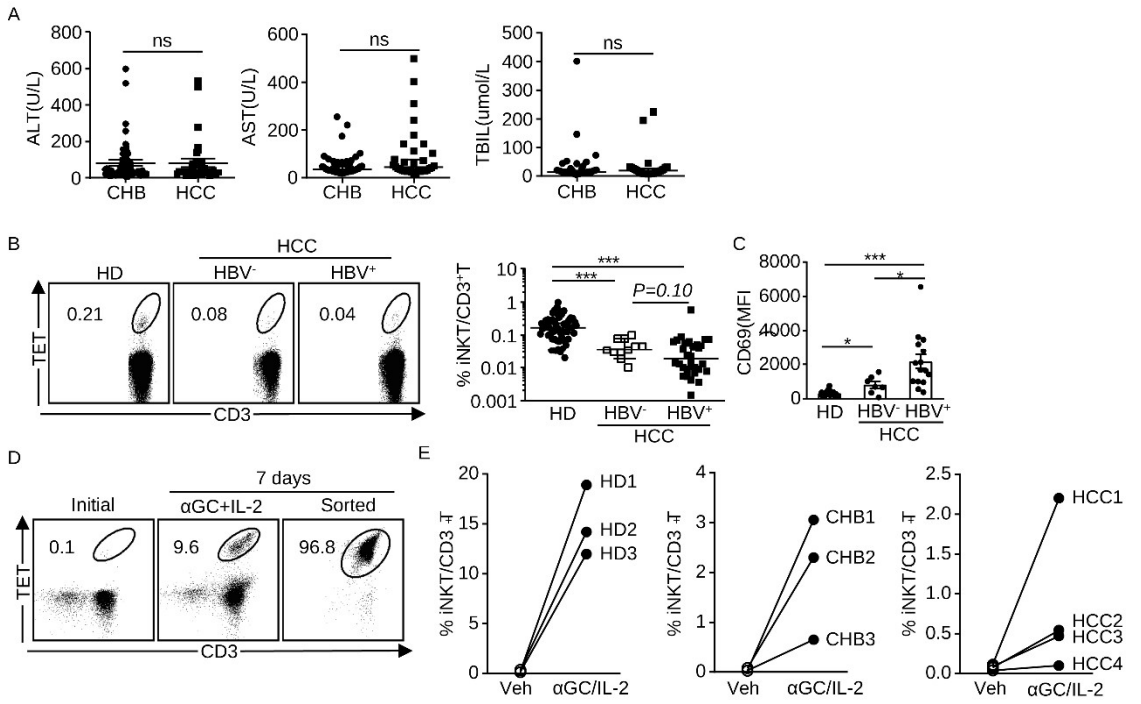

Supplementary Fig. S1. HBV-related HCC patients have similar degrees of liver injury as CHB patients, while their iNKT cells are hyperactivated but impaired in α-GalCer-induced expansion.

(A) The level of ALT, AST, and TBIL of Chronic hepatitis B (CHB) patients (n=54) and HBV-related HCC (HCC) patients (n=32) are shown. (B) Representative dot plots and summary scatter graph depict the ratio of circulating iNKT cells in $CD3^+$ T cells from the peripheral blood from healthy donors (HD, n=56), HBV negative HCC (HBV^- HCC, n=11), and HBV-related HCC patients (HBV^+HCC, n=32, the same to Figure 1A). Data are shown as median with 95%CI, and the statistical significance between groups was determined by Mann-Whitney U-test. (C) Bar graph with scatter plots depicts CD69 levels on iNKT cells from indicated groups. (n=7-25/group). Data are shown as mean ± SEM and the statistical significance was determined by an unpaired two-tailed Student's t-test. *$p < 0.05$, ***$p < 0.001$. (D) Representative dot plots show frequencies of initial, α-GalCer/IL-2-expanded (αGC/IL-2), and sorted iNKT cells in PBMCs from healthy donor. (E) PBMCs from healthy donors (HD1-3), chronic HBV infection patients (CHB1-3), and HBV-related HCC patients (HCC1-4) were stimulated by α-GalCer/IL-2 (αGC/IL-2) for 7 days. Scatter plots show the ratios of iNKT cells from indicated individuals stimulated by vehicle or αGC/IL-2.

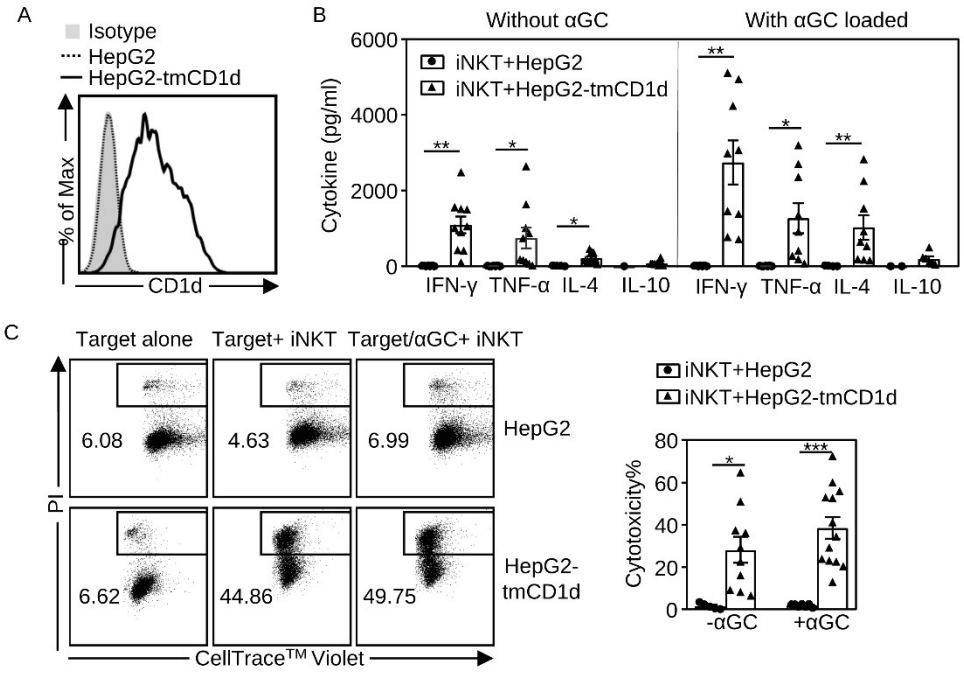

Supplementary Fig. S2. Human iNKT cells produce Th1-biased cytokines and exhibit cytotoxicity against hepatoma cells in a CD1d-dependent way.

PBMCs from the healthy donor were stimulated by α-GalCer (αGC) and IL-2 for 7 days. PBS57/hCD1d-tetramer (TET) sorted iNKT cells were stimulated with HepG2 or HepG2-tmCD1d without or with α-GalCer loaded. (A) Representative histogram for CD1d expression on HepG2 and HepG2-tmCD1d. (B) Concentrations of IFN-γ, TNF-α, IL-4, and IL-10 in indicated groups (n=4-10/group). (C) CellTraceTM Violet-labeled HepG2 and HepG2-tmCD1d were pulsed with vehicle (-αGC) or α-GalCer (+αGC) and then co-cultured with sorted iNKT cells. Target cells alone served as control. iNKT cells cytotoxicity was analyzed by measuring the percentage of Propidium Iodide (PI) staining target cells. Representative dot plots (left panel) and summarized cytotoxicity% (right panel) are shown (n=5-13/group). Data are shown as mean ± SEM and the statistical significance was determined by an unpaired 2-tailed Student's t-test. *$p < 0.05$, **$p < 0.01$, ***$p < 0.001$.

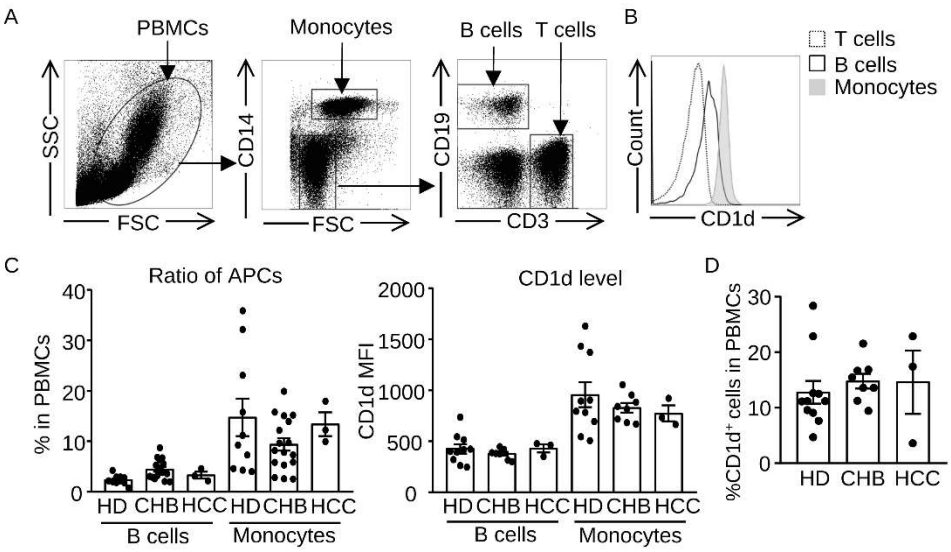

Supplementary Fig. S3. No changes in CD1d-expressing cells in peripheral blood from CHB and HCC patients.

(A)Representative dot plots for gating strategy for monocytes, B cells and T cell in PBMCs. (B)Histogram shows CD1d levels in indicated cell populations. (C) Percentages and CD1d levels of circulating B cell and monocyte in indicated groups. (D) Percentages of CD1d-expressing cells in PBMCs from indicated groups. Bar graphs are shown as mean ± SEM. Data are pooled from at least 3 independent experiments.

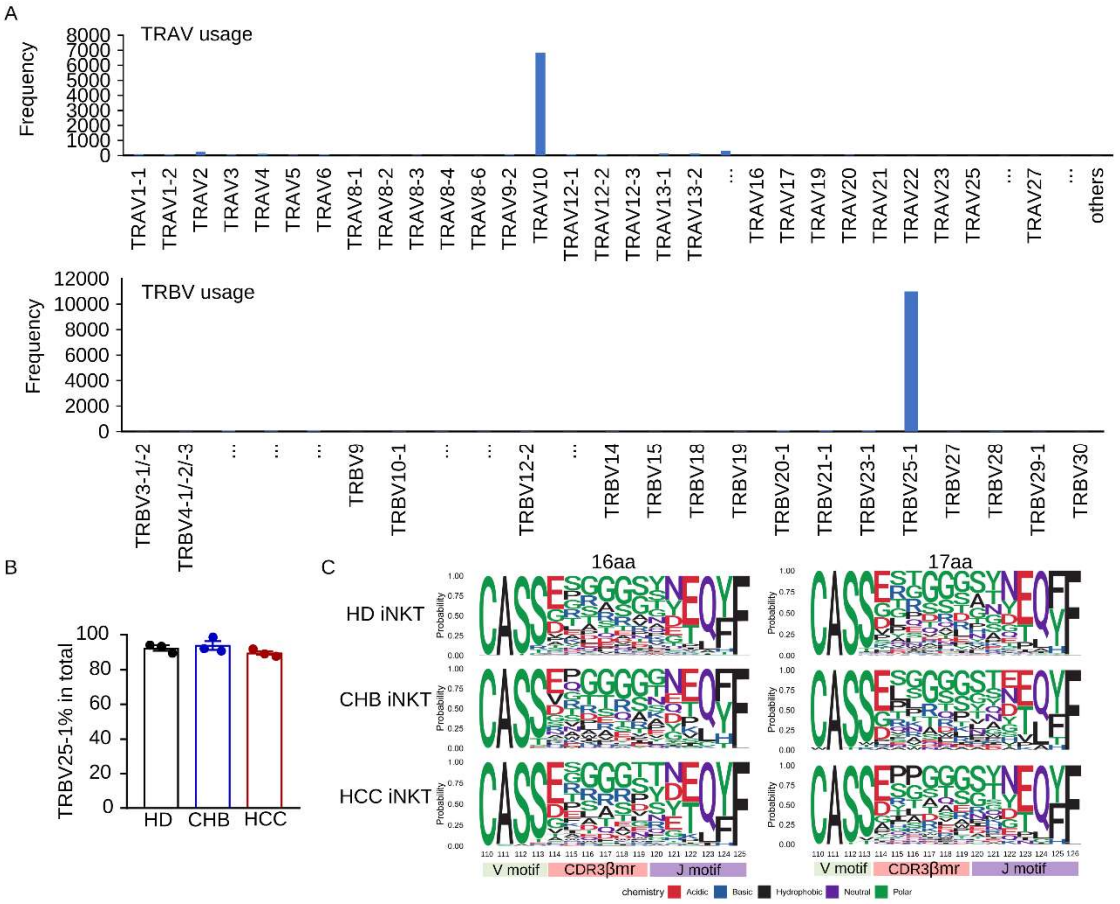

Supplementary Fig. S4. iNKT cells from different individuals typically express an invariant TRAV10-TRAJ18 and highly diverse TCR CDR3β loop.

RNA sequencing data of α-GalCer/IL-2 expanded iNKT cells from 3 HD (HD1-3, HD iNKT), 3 CHB (CHB1-3, CHB iNKT), and 3 HCC patients (HCC1-3, HCC iNKT) were analyzed for TCR usages by MiXCR software. (A) The frequency of TRAV and TRBV usage of iNKT cells from all detected individuals. (B) The percentage of TRBV25-1 in iNKT cells from indicated groups. (C) Seqlogo plots for amono acid enrichment at each position for CDR3β sequences in indicated groups (n=3/group).

A

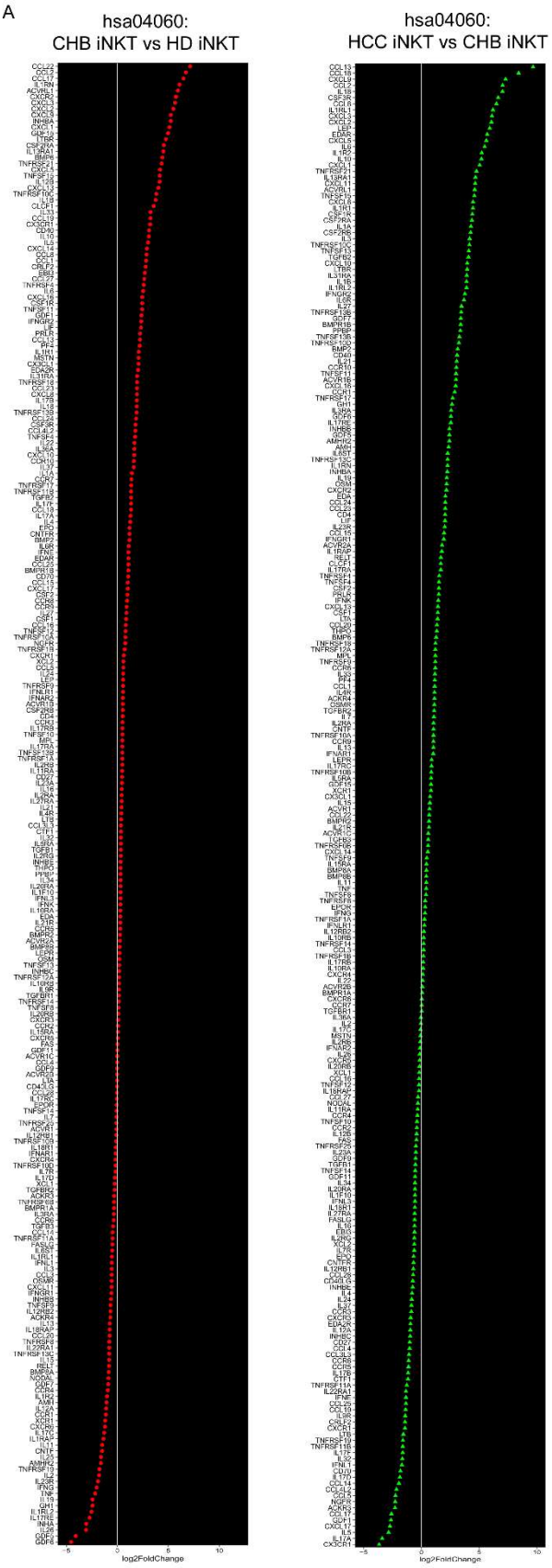
hsa04060:
CHB iNKT vs HD iNKT
hsa04060:
HCC iNKT vs CHB iNKT
log2FoldChange
log2FoldChange

B

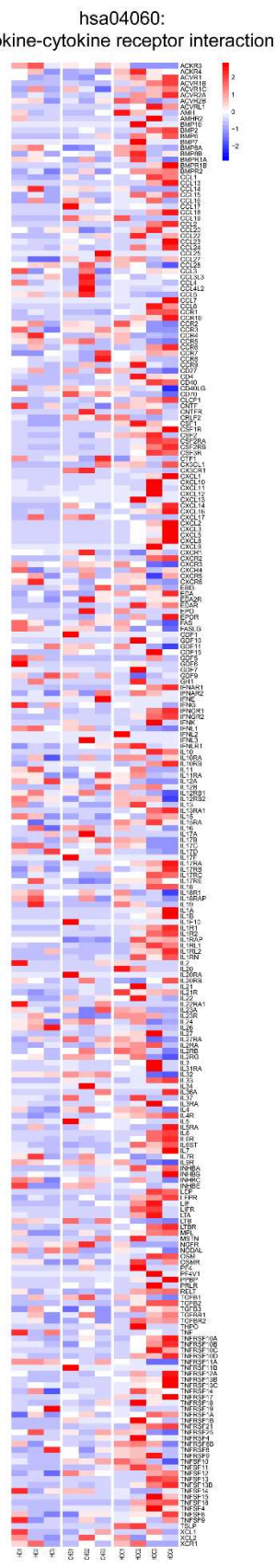
hsa04060:
Cytokine-cytokine receptor interaction

Supplementary Fig. S5. HCC iNKT cells have predominantly increased genes in the 'Cytokine-cytokine receptor interaction' pathway.
(A) Plot showing the Log2 fold change value of genes of 'Cytokine-cytokine receptor interaction' pathway in CHB iNKT vs HD iNKT (left panel) and HCC iNKT vs CHB iNKT (right panel). (B) Heatmap of the relative levels of involved genes in indicated samples.

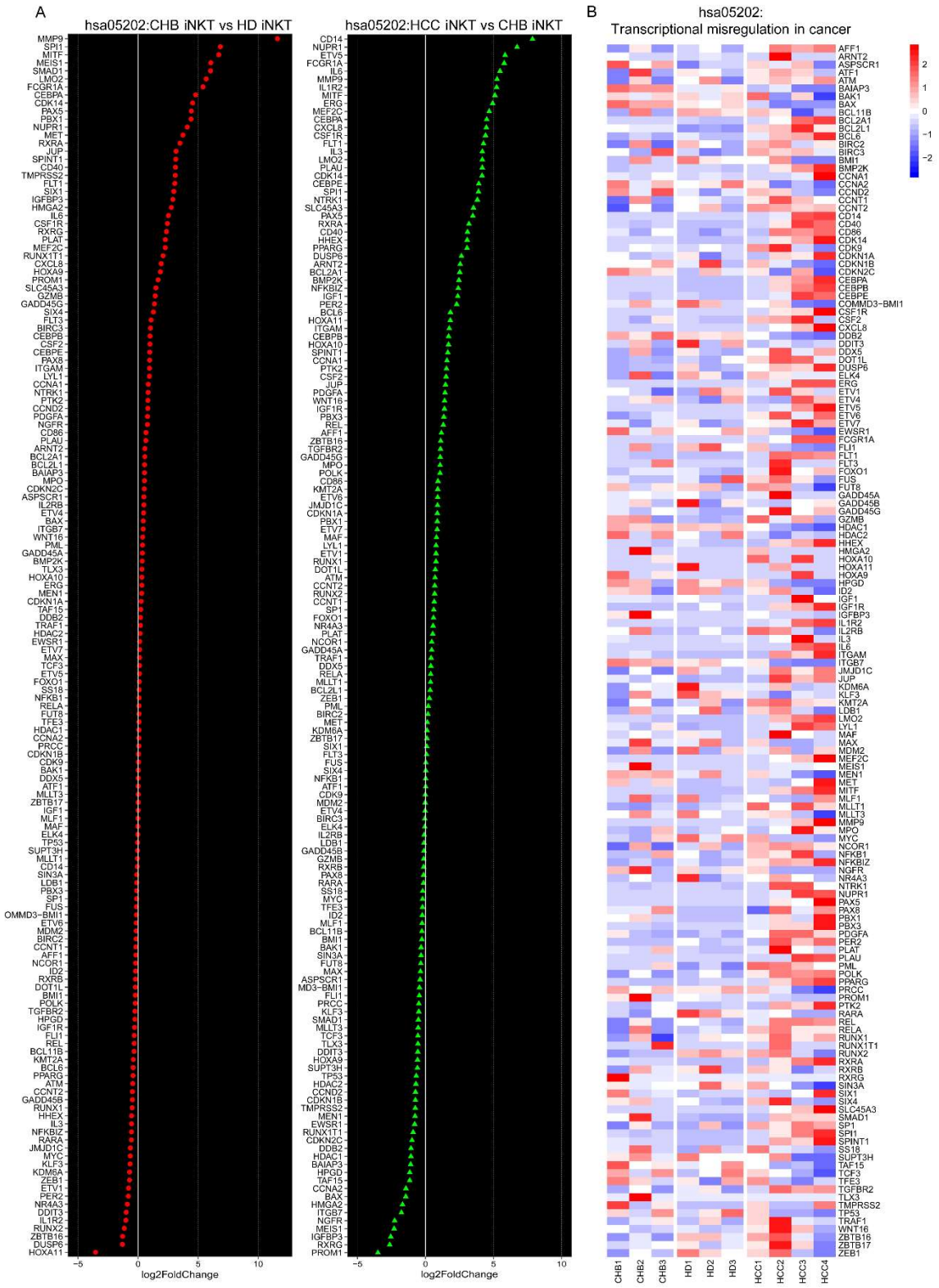

Supplementary Fig. S6. HCC iNKT cells have predominantly increased genes in the 'Transcriptional misregulation in cancer' pathway.

(A) Plot showing the Log2 fold change value of genes of 'Transcriptional misregulation in cancer' pathway in CHB iNKT vs HD iNKT (left panel) and HCC iNKT vs CHB

iNKT (right panel). (B) Heatmap of the relative levels of involved genes in indicated samples.

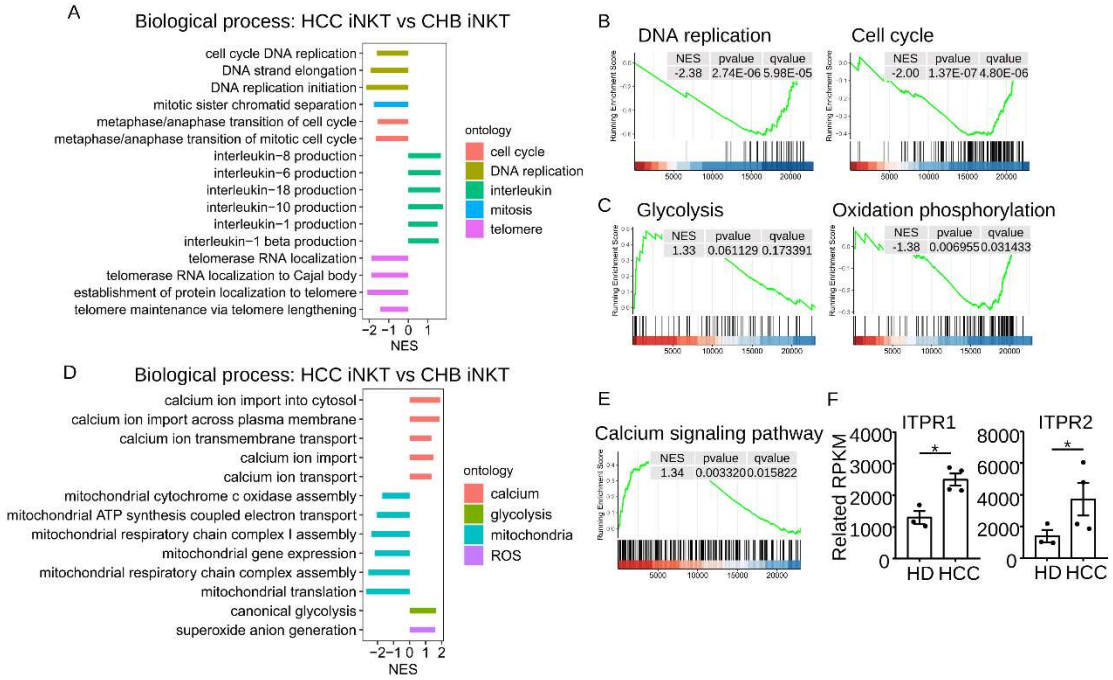

Supplementary Fig. S7. iNKT cells from HBV-related HCC patients present an elevated senescent phenotype compared to chronic hepatitis B patients.

Transcripts from RNA-Seq data of GalCer/IL-2 expanded iNKT cells from HCC (HCC1-4, n=4) and CHB patients (CHB1-3, n=3) were compared and enriched for GO, KEGG, and GSEA analysis. (A) The histogram graph shows normalized enrichment scores (NES) of senescence-related biological processes from GSEA analysis based on the GO database. (B) GSEA of the transcriptional signature of “DNA replication” and “Cell cycle” KEGG pathways. (C) GSEA of the transcriptional signature of “Glycolysis” and “Oxidation phosphorylation” KEGG pathway. (D) The histogram graph shows normalized enrichment scores (NES) of telomere maintenance-, calcium transport-, and mitochondrial function–related biological processes from GSEA analysis based on the GO database. (E) GSEA of the transcriptional signature of the “Calcium signaling pathway” KEGG pathway. (J) Scatter graphs with bar show related mRNA levels of *ITPR1 and ITPR2* in the indicated groups. Data are shown as mean ± SEM and the statistical significance was determined by DESeq on R.

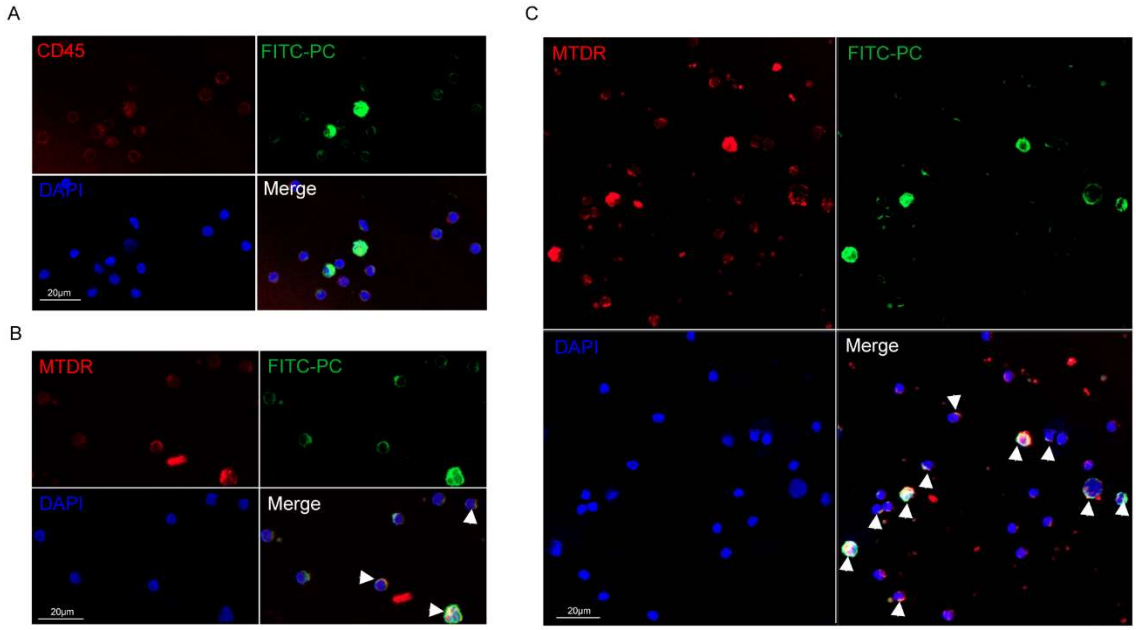

Supplementary Fig. S8. Colocalization of PC and the mitochondrial tracker are frequently found in immune cells.
(A) Confocal image shows the localization of FITC-PC in the lymphocytes that stained with CD45. (B-C) Confocal image shows the localization of FITC-PC in the lymphocytes that stained with mitochondrial deep red (MTDR).

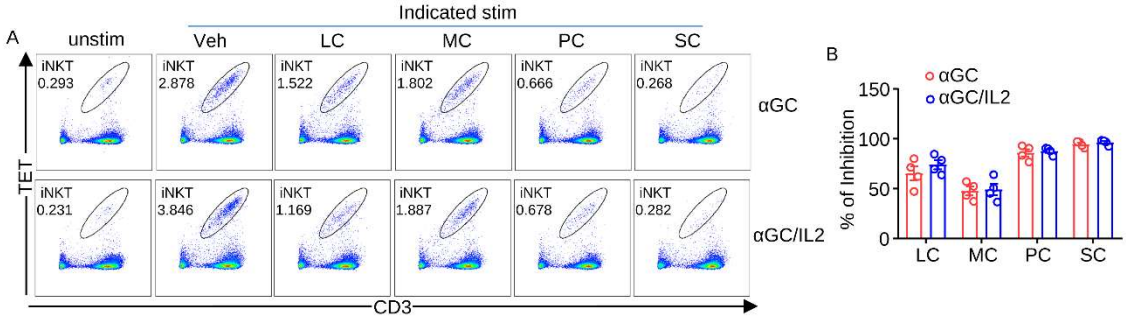

Supplementary Fig. S9. Similar inhibitory effects of LCACs on α-GalCer-expanded iNKT cells and α-GalCer/IL-2-expanded iNKT cells.

PBMCs from healthy donors were stimulated with α-GalCer and LCACs in the absence (aGC) or presence IL-2 (aGC/IL-2) for 7 days, followed by iNKT cell detection. Representative dot plots (A) and bar graph with scatter plots (B) show the ratio of iNKT cells and inhibition rates, respectively.

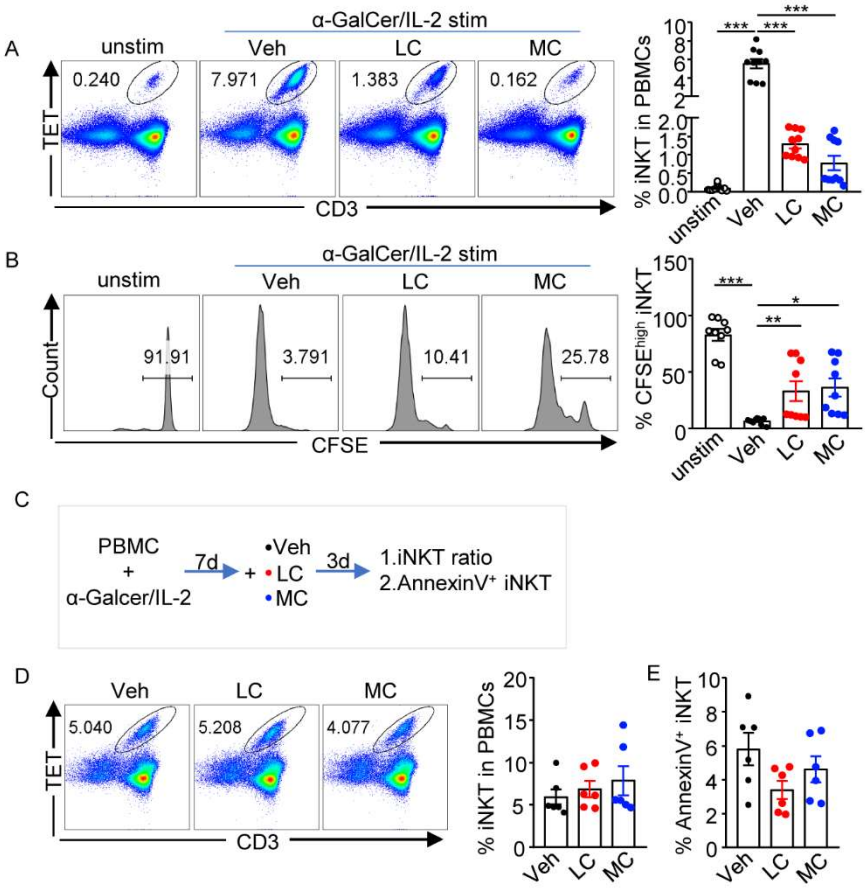

Supplementary Fig. S10. Lauroyl-carnitine and myristoyl-carnitine impair α-GalCer/IL-2-induced iNKT cell proliferation.

(A-D) PBMCs from healthy donors were stimulated with α-GalCer/IL-2 for 7 days in the presence of vehicle (Veh), lauroyl-carnitine (LC), or myristoyl-carnitine (MC). (A) Representative dot plots and bar graph with scatter plots show the percent of iNKT cells in PBMCs treated with vehicle (Veh), LC (100 μM), or MC (100 μM) (n=10/group). (B) Representative histograms and the bar graph with scatter plots show the percent of $CFSE^{high}$ iNKT cells in indicated groups (n=9/group). (C-E) PBMCs from healthy donors were stimulated with α-GalCer/IL-2 for 7 days and then treated with vehicle (Veh), LC (100 μM), or MC (100 μM) for 3 days. (C) The flow chart shows the process of the assay. (D) Representative dot plots and bar graph with scatter plots show the percent of iNKT cells in PBMCs in indicated groups (n=6/group). (E) The bar graph with scatter plots shows the percent of $annexinV^+$ iNKT cells in indicated groups (n=6/group). Data are shown as mean ± SEM and the statistical significance was determined by a paired 2-tailed Student's t-test. *$p < 0.05$, **$p < 0.01$, ***$p < 0.001$.

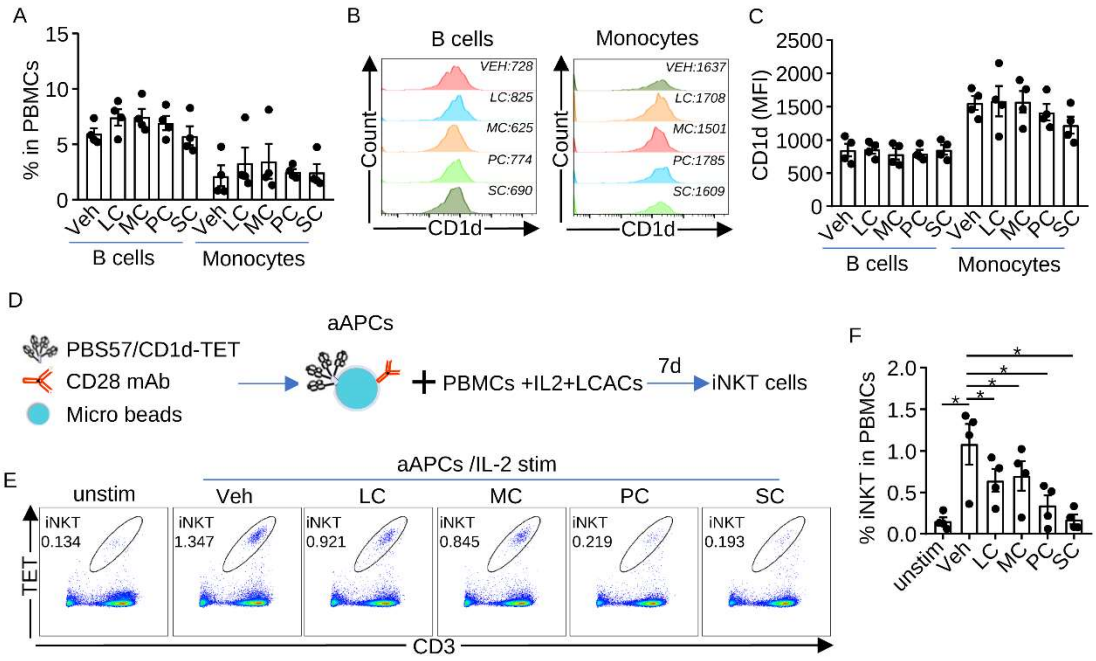

Supplementary Fig. S11. The inhibition to iNKT expansion mediated by LCACs was independent of altered a-GalCer presentation by APCs.

(A-C) PBMCs from healthy donors (n=4) were stimulated with α-GalCer/IL-2 in the presence of LCACs for 3 days, followed by the detection of ratios and CD1d-expression levels of B cells and monocytes. (A) Summary bar graph with scatter plots shows the ratio of B cells and monocytes in PBMCs in indicated groups. (B) Histograms and (C) summary bar graph with scatter plots show the CD1d levels of B cells and monocytes in indicated groups. (D-F) PBMCs were stimulated with microbeads coating with PBS57/hCD1d tetramer and anti-CD28 antibody in the presence of different LCACs. (D) The flow chart shows the experimental design. (E) Representative dot plots and (F) summary bar graph with scatter plots show the percent of iNKT cells in PBMCs. Bar graphs are shown as mean ± SEM. Data are statistical significance determined by a paired 2-tailed Student's t-test. *P < 0.05.

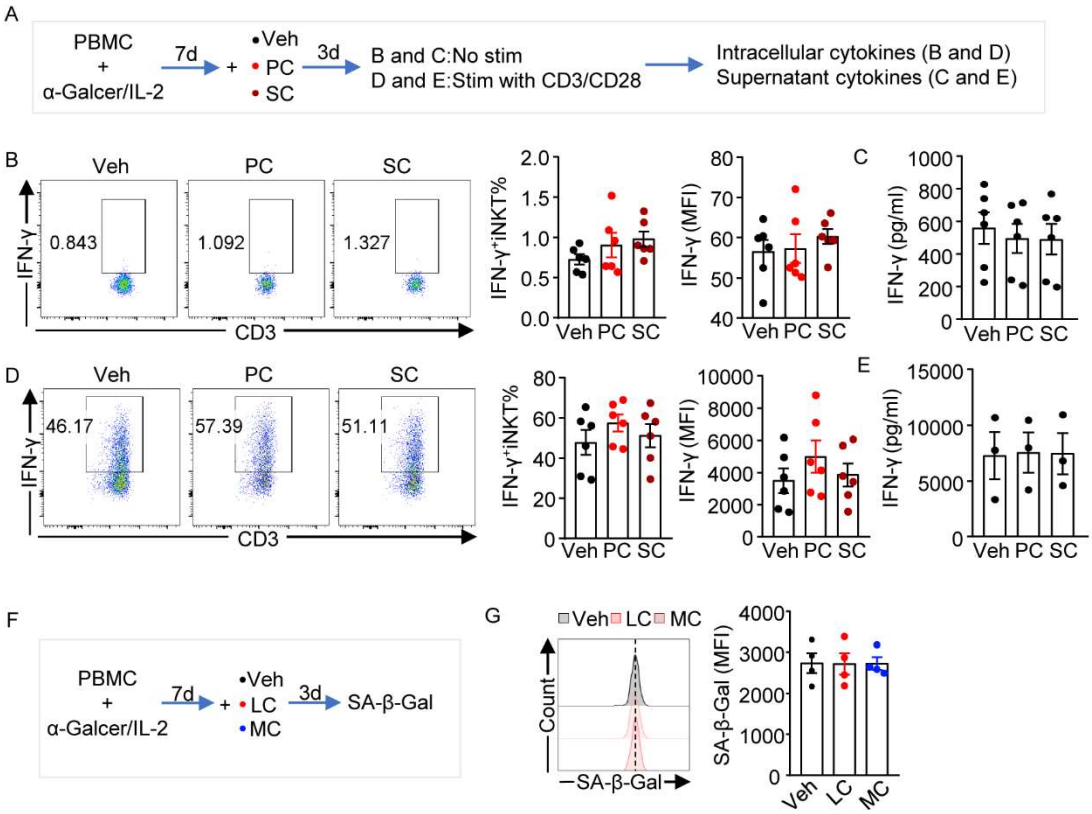

Supplementary Fig. S12. Accumulation of LCACs do not lead to deficiency in IFN-γ production of iNKT cells and show little effect in promoting senescent phenotype.
PBMCs from healthy donors were stimulated with α-GalCer/IL-2 for 7 days, and treated with vehicle (Veh), palmitoyl-carnitine (PC) or stearoyl-carnitine (SC) for 3 days, followed by a CD3/CD28 stimulation or not for the intracellular cytokines and supernatant cytokines detection. (A) The flow chart shows the process of the assay. (B) Representative dot plots and summary bar graphs with scatter plots show the percent of IFN-γ+ iNKT cells and IFN-γ mean fluorescence intensity (MFI) of iNKT cells in indicated groups without CD3/CD28 stimulation (n=6/group). (C) The concentration of IFN-γ in the supernatant of PBMCs without CD3/CD28 stimulation (n=6/group). (D) Representative dot plots and summary bar graphs with scatter plots show the percent of IFN-γ+ iNKT cells and IFN-γ MFI of iNKT cells in indicated groups with CD3/CD28 stimulation (n=6/group). (E) The concentration of IFN-γ in the supernatant of PBMCs without CD3/CD28 stimulation (n=6/group). (F-G) PBMCs from healthy donors were stimulated with α-GalCer/IL-2 for 7 days and then treated with vehicle (Veh), LC (100 μM), or MC (100 μM) for 3 days. (F) The flow chart shows the process of the assay. (G) Representative dot plots and bar graph with scatter plots show the SA-β-Gal levels of iNKT cells in indicated groups (n=4/group).Data are shown as mean ± SEM pooled from 3 independent experiments.

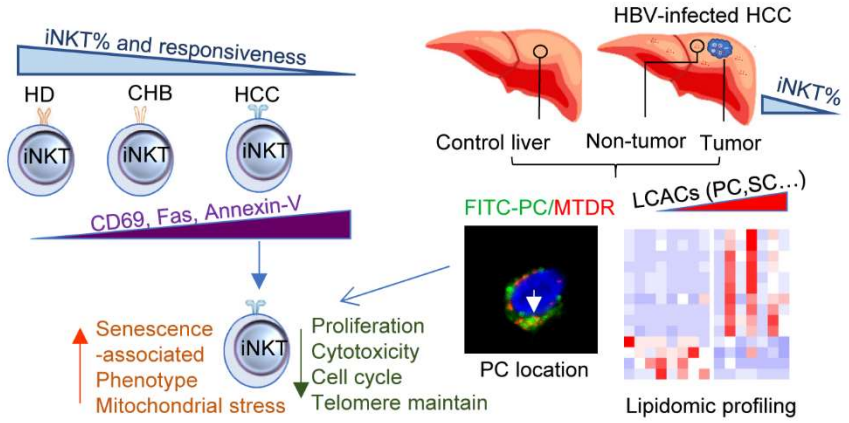

Supplementary Fig. S13. INKT cells senescence correlates with accumulated LCACs in HBV-related HCC.